Novel technique for the wireless reading of passive microfluidic sensors

Dominique Henry, Hervé Aubert, Patrick Pons, J. Lorenzo, A Lázaro, D Girbau

Novel technique for the wireless reading of passive microfluidic sensors.

D. Henry, H. Aubert, P. Pons, J. Lorenzo, A. Lázaro and D. Girbau

This letter focuses on the remote reading of high-resolution microfluidic and passive (i.e., batteryless and chipless) temperature sensors. These sensors are remotely interrogated from a 24GHz Frequency-Modulated Continuous-Wave radar performing a mechanical beam scanning for locating the sensors and measuring the variation of sensors electromagnetic echo level due to temperature fluctuation. From radar measurement data an estimator is proposed here for determining the meniscus position of the fluid inside the sensors microchannel and for deriving the temperature at the sensors location. It is shown that the estimator presents a convenient linear dependence with the meniscus position at the sensor location. The smallest measurable variation of the meniscus position is of 40µm.

Introduction: Nowadays the wireless reading of passive sensors is still a very challenging issue to overcome. In order to render such sensors competitive compared to the active sensors, two main technical improvements must be performed: (1) increasing the reading range to reach significantly more than few meters and, (2) achieving higher measurement resolution. As a matter of fact the typical interrogation range achievable by sensors integrated in Radio-Frequency Identification (RFID) tags does not exceed few meters and the typical long-range qualification for batteryless RFID tags is around 12 meters [1, 2]. Moreover passive sensors using an electromagnetic transduction (see, e.g., [3-5]) allow higher reading range (up to some decameters [6]) but suffer from poor measurement resolution of the physical or chemical quantity of interest compared to their active counterpart.

In this Letter we report for the first time a wireless reading technique for improving the measurement resolution of wireless, batteryless and chipless sensors. The technique is applied here for the remote interrogation of the passive microfluidic temperature sensors reported in [7]. This novel technique consists of performing the mechanical scanning of the monostatic FM-CW radar antenna main lobe in order to locate the sensor in the 3D illuminated scene and to compute an estimator for remotely deriving the temperature at the sensor location. Unlike previously reported approaches (see, e.g., [6]) this estimator is not only computed from the beat frequency spectrum obtained in the sensor direction but, from the appropriate combination of numerous spectra measured in many directions around the sensor direction.

After a very brief reminder of the microfluidic sensor design reported in [7] the Letter describes the proposed radar beam scanning technique for the sensor detection and wireless reading. The last section focuses on the remote estimation of the meniscus position of the fluid (water) inside the sensors microchannel by the original combination of multiple beat frequency spectra. The temperature resolution of the microfluidic sensor is finally estimated.

Principle of the Wireless Reading of Passive Sensors: Recently some of us have reported the design of a passive sensor using a fluidic microchannel within a gap of an impedance matched microstrip transmission line [7]. Due to the dilatation coefficient of the liquid (water), the meniscus position of the fluid inside the microchannel is modified as the temperature changes at the gap location. The temperature-dependent gap capacitance is designed on a 525µm B33 glass wafer metalized both sides with 0.5µm aluminium. A top view of the microchannel is shown on Fig. 1. The fluidic microchannel is located in the gap of the microstrip transmission line of length of 1.4cm which propagates only the fundamental mode at 24GHz. This line is impedance matched (50Ω) at one port and is connected to a horn antenna via a delay line (effective length of 1.8m) at its other port. A pressure monitoring system controls the meniscus position of the water inside the sensor microchannel.

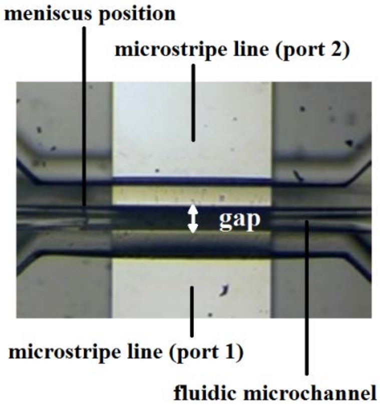

Fig. 1 *Top view of the fabricated microfluidic temperature sensor (detail).*

The position of the fluid meniscus inside the microchannel may be wirelessly derived from pointing the main lobe of a monostatic radar antenna in the direction of the sensor and measuring the echo level, as reported in [7]. However the resulting measurement sensitivity is significantly degraded when the main lobe direction is slightly changed. In order to overcome this critical issue, the mechanical scanning of the monostatic FM-CW radar antenna main lobe is proposed here in order to obtain a 3D radar image. In many directions around the sensor position, the radar transmits a chirp at a carrier frequency of 23.8GHz with a triangular frequency modulation band of 2GHz (sweep rate of 400MHz/ms). This bandwidth provides a theoretical depth resolution of 7.5cm. At the front-end of the radar are connected a parabolic antenna (Tx-antenna) and a 1x4 patch array antenna (Rx-antenna). The Tx-antenna has a narrow beamwidth of 2° and a high gain of 33.5dBi. The Rx-antenna has a beamwidth of 60° in azimuth and 25° in elevation. Antennas and FM-CW radar are mounted on a rotating platform in order to point the Tx-antenna main lobe in controlled directions. The azimuth and elevation sweeps of ±10° of the Tx-antenna main lobe with an angular resolution of 1° are applied here. The sensor antenna is located at 2.5m in front of the radar while the effective length between the radar and the fluidic microchannel (including the delay line) is of 4.3m. Unwanted echoes (clutters) may hide the electromagnetic backscattering from the sensor. In order to avoid this undesirable effect the length of the delay line is adjusted in order to locate the desired sensing backscattering mode in a region without clutters.

Measurement results and discussion: Fig. 2 shows the obtained 3D radar image resulting from the FM-CW radar beam scanning technique when the microchannel is empty and when the water completely fills the gap. (Fig. 2 does not include the electromagnetic echo from the sensor antenna). This image, obtained from the pointing of the Tx-antenna main lobe in 441 directions, is composed of 33624 voxels of 11.4 cm^3. It can be conveniently analysed by computing the so-called *isosurfaces* [8], that is, sets of superimposed 3D contours sharing the same echo level. When the microchannel is empty, the number of voxels for which the echo level is higher than a given threshold (here of -20dB) is found to be larger than the number of voxels obtained when the water completely fills the gap. This was expected because the fluidic microchannel in the gap behaves mainly as a series capacitance: when the gap is completely filled with water the measured series capacitance is of 150fF and is higher than the series capacitance (100fF) of the empty microchannel. More microwave power is then transmitted through the gap and more power is dissipated in the 50Ω loading impedance. As a consequence less power is available for the sensor electromagnetic backscattering. This is the reason why the number of voxels when the gap is empty is larger than the number of voxels obtained when the water completely fills the gap. Note that the threshold value (-20dB) was chosen here to facilitate the analysis of 3D radar images obtained for various meniscus positions. The number of voxels for which the echo level is higher than the threshold is a function of the quantity of fluid inside the microchannel or, in other words, is dependent on the position of the fluid meniscus in the microchannel.

From this number of voxels a convenient parameter or estimator is now defined for deriving the fluid meniscus position from the radar measurement data.

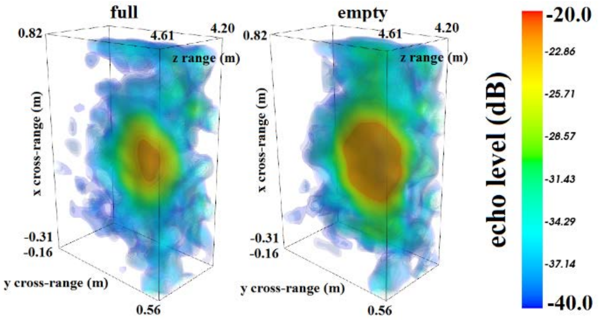

Fig. 2 *3D representation of the microfluidic sensor echo when the gap is completely filled with water (left) or empty (right). The electromagnetic echo from the sensor antenna is not present in the 3D region considered in the Figure.*

The proposed beam scanning technique allows selecting the voxel for which the echo level is maximal in the 3D radar image of the microfluidic sensor. This echo is used here as an estimator of the temperature-dependent position of the fluid meniscus in the microchannel. In Fig. 3 the echo is displayed as a function of the position of the fluid (water) meniscus in the microchannel. From minimizing the squared distance between the echo and a regression line (ordinary least square regression technique), a convenient linear model is derived with a coefficient of determination R^2 of 0.932. The slope of the regression line –or equivalently, the sensibility of the estimator to meniscus position– is of 6dB/mm. The maximal echo level may also be displayed as a function of the microfluidic gap capacitance. The resulting linear model yields to a sensitivity of 0.12dB/pF, that is, a value significantly higher than the sensitivity (0.03dB/pF) obtained from the wireless interrogation technique reported in [7] based on radar echoes obtained only in the sensor direction.

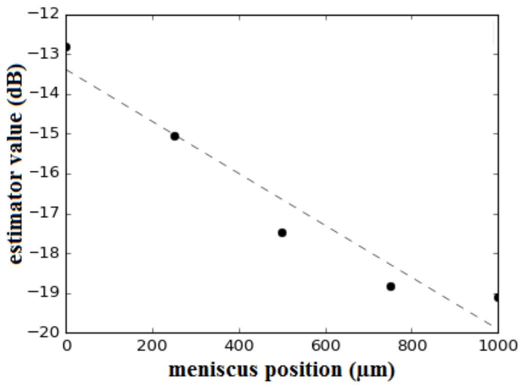

Fig. 3 *Estimator of the temperature-dependent position of the fluid (water) meniscus in the microchannel as a function of the meniscus position (0µm: the gap is empty; 1000µm: the water completely fills the gap). This estimator is the highest echo level value detected in the 3D radar image of the microfluidic sensor. The linear model built from 5 meniscus positions has a slope of -6dB per mm with a coefficient of determination R²=0.932 and a standard error of 0.3dB.*

The precision of the estimator, that is, the smallest measurable variation ΔL of the meniscus position, is found to be of 40 µm when applying the proposed beam-scanning technique (it is of 60 µm when applying the wireless technique reported in [7]). The resulting smallest measurable temperature variation ΔT is then derived as follows:

$$\Delta T = \frac{S_c}{\alpha\, V_{tank}} \Delta L \qquad (1)$$

where α designates the dilatation coefficient of the water, V_{tank} (= 3mm^3) denotes a cylindrical tank volume and S_c (=0.015µm^2) is the cross-section area of the microfluidic channel. The dilatation coefficient α of water ranges from 247ppm/°C to 385ppm/°C between 24.0°C and 40.0°C but, for the sake of simplification, this variation is not considered here and the dilatation coefficient α is taken at the initial ambient temperature of 24°C). Consequently, from (1) one derives ΔT=0.8°C. The microchannel is completely filled at a temperature of 37.6°C. The full-scale temperature range is then of 13.6°C and the temperature measurement resolution is of 6% of the full-scale measurement range. This is a significant improvement compared with our previous work [7] in which the temperature resolution was of 14% of full-scale range.

Conclusion: The radar beam scanning technique applied to the remote detection and reading of passive microfluidic sensor allows the estimation of the temperature at the sensors location with a temperature measurement resolution of 6% of the full-scale range. The sensor is remotely interrogated from a 24GHz Frequency-Modulated Continuous-Wave radar. By defining an appropriate estimator, a linear model for deriving the variation of the meniscus position of the fluid in the microchannel is reported, with a sensitivity of -6dB per mm. The smallest measurable variation of the meniscus position is found to be of 40µm. Preliminary measurement results (not yet published) indicate that the proposed radar beam scanning technique allows reading passive sensors up to 60 meters. Next step consists of exploring the practical and theoretical limitations of the proposed radar beam scanning approach in terms of measurement resolution, precision and reading range.

D. Henry, H. Aubert and P. Pons (*LAAS-CNRS, Toulouse, 31031 France*)
E-mail: dhenry@laas.fr
J. Lorenzo, A. Lázaro and D. Girbau (*Universitat Rovira i Virgili, Tarragona, 43007 Spain*)

References

1. Lee, K.K., Lande, T.S.: 'A Wireless-Powered IR-UWB Transmitter for Long-Range Passive RFID Tags in 90-nm CMOS', *IEEE Trans. on Circuits and Systems II: Express Briefs*, 2014, **61**, (11), pp. 870-874, doi: 10.1109/TCSII.2014.2350292
2. Park, I.Y., Kim, D.: 'Artificial magnetic conductor loaded long-range passive RFID tag antenna mountable on metallic objects', *Electronics Letters*, 2014, **50**, (5), pp. 335-336, doi: 10.1049/el.2013.2671
3. Hester, J.G.D, Tentzeris, M.M.: 'Inkjet-Printed Flexible mm-Wave Van-Atta Reflectarrays: A Solution for Ultralong-Range Dense Multitag and Multisensing Chipless RFID Implementations for IoT Smart Skins', *IEEE Trans. on Microwave Theory and Techniques*, 2016, **64**, (12), pp. 4763-4773, doi: 10.1109/TMTT.2016.2623790
4. Henry, D., Aubert, H., Pons, P.: '3D scanning and sensing technique for the detection and remote reading of a passive temperature sensor', *2016 IEEE MTT-S International Microwave Symposium (IMS),* San Francisco, CA, 2016, pp. 1-4, doi: 10.1109/MWSYM.2016.7540414
5. Tan, Q., Luo, T., Wei, T., Liu, J., Lin, L., Xiong, J., 'A Wireless Passive Pressure and Temperature Sensor via a Dual LC Resonant Circuit in Harsh Environments', *Journal of Microelectromechanical Systems*, 2017, **26**, (2), pp. 351-356, doi: 10.1109/JMEMS.2016.2642580
6. Aubert, H., Chebila, F., Jatlaoui, M., Thai, T., Hallil, H., Traille, T., Bouaziz, S., Rifai, A., Pons, P., Menini, P., Tentzeris, M.M. : 'Wireless Sensing and Identification based on RADAR Cross Sections Variability Measurement of Passive Electromagnetic Sensors', 2013, *Annals of Telecommunications Springer*, **68**, (7-8), pp.425-435, doi: 10.1007/s12243-013-0376-5
7. Bouaziz, S., Chebila, F., Traille, A., Pons, P., Aubert, H., Tentzeris, M.M.: 'Novel Microfluidic Structures for Wireless Passive Temperature Telemetry Medical Systems Using Radar Interrogation Techniques in Ka-Band', *IEEE Antennas and Wireless Propagation Letters*, 2012, **11**, pp. 1706-1709, doi: 10.1109/LAWP.2013.2242272
8. Ramachandran, P., Varoquaux, G., 'Mayavi: 3D Visualization of Scientific Data', *IEEE Computing in Science & Engineering*, 2011, **13**, (2), pp. 40-51, doi: 10.1109/MCSE.2011.35